(28) Provencher, S. W. *Makromol. Chem.* **1979**, *180*, 201.
(29) Provencher, S. W.; Hendrix, J.; de Maeyer, L.; Paulsson, N. J. *Chem. Phys.* **1978**, *69*, 4273.
(30) Klein, J.; Fletcher, D.; Fetters, L. J. *Nature (London)* **1983**, *304*, 526.
(31) Bartels, C. R.; Crist, B., Jr.; Fetters, L. J.; Graessley, W. W. *Macromolecules* **1986**, *19*, 785.
(32) Antonietti, M.; Sillescu, H. *Macromolecules* **1986**, *19*, 798.
(33) Daoud, M.; de Gennes, P.-G. *J. Polym. Sci., Polym. Phys. Ed.* **1979**, *17*, 1971.
(34) Klein, J. *Macromolecules* **1981**, *14*, 460.
(35) Graessley, W. W. *Adv. Polym. Sci.* **1982**, *47*, 67.
(36) Fujita, H.; Einaga, Y. *Polym. J. (Tokyo)* **1985**, *17*, 1131.
(37) von Meerwall, E.; Tomich, D. H.; Hadjichristidis, N.; Fetters, L. J. *Macromolecules* **1982**, *15*, 1157.
(38) von Meerwall, E.; Tomich, D. H.; Grigsby, J.; Pennisi, R. W.; Fetters, L. J.; Hadjichristidis, N. *Macromolecules* **1983**, *16*, 1715.
(39) Lodge, T. P.; Wheeler, L. M. *Macromolecules* **1986**, *19*, 2983.
(40) Grubisic, Z.; Rempp, P.; Benoit, H. *J. Polym. Sci., Polym. Lett. Ed.* **1975**, *5*, 753.
(41) Muthukumar, M.; Baumgartner, A. *Macromolecules* **1989**, *22*, 1937, 1941.

Registry No. Polyisoprene, 9003-31-0; polystyrene, 9003-53-6.

Effect of Water on Diblock Copolymers in Oil: Large Aggregates, Micelles, and Microemulsions

Kathleen A. Cogan and Alice P. Gast*

Department of Chemical Engineering, Stanford University, Stanford, California 94305.
Received April 20, 1989; Revised Manuscript Received July 5, 1989

ABSTRACT: We present a dynamic light scattering study of polystyrene–poly(ethylene oxide) diblock copolymers in cyclopentane, a selective solvent for polystyrene. We find that a trace amount of water has a profound effect on the structures formed in dilute solution due to the compatibility of poly(ethylene oxide) and water. We investigate changes in hydrodynamic radius as a function of copolymer and water concentration for two diblock copolymers of varying composition and molecular weight. Unusually large stable aggregates form in solutions with low water content. Addition of water promotes monodisperse spherical micelles in solutions of large aggregates as well as in solutions containing only single chains. Further addition of water results in a solution of swollen micelles, i.e., a polymeric microemulsion. At very low copolymer concentrations, saturated micelles exhibit a sharp increase in hydrodynamic size.

Introduction

Block copolymers in a selective solvent can form structures due to their amphiphilic nature. Above the critical micelle concentration (cmc), the free energy of the system is lower if the block copolymers associate into micelles rather than remain dispersed as single chains. Often the micelles are spherical, with a compact core of insoluble blocks surrounded by a corona of soluble blocks.[1-3] Addition of a second solvent, compatible with the insoluble block and immiscible with the continuous phase, leads to the formation of swollen micelles or a polymeric microemulsion.

In this paper, we describe the effects of changing water and copolymer concentrations for polystyrene–poly(ethylene oxide) (PS–PEO) diblock copolymers in cyclopentane at 23 °C. Since water is a solvent for poly(ethylene oxide) and cyclopentane is a near Θ solvent for polystyrene (T_Θ = 19.5 °C)[4], the micelles consist of a poly(ethylene oxide) core swollen with water and protected by a polystyrene corona. Previous morpholigical studies of polymeric microemulsions have involved graft and block copolymers in ternary solvent mixtures containing toluene, water, and either an alcohol or an amine acting as a cosurfactant.[5-9] Although the cosurfactant increases the dispersion capability of the copolymers, it adds to the complexity of the system since it is generally soluble in both the continuous and dispersed phases. We investigate the dispersion of water in cyclopentane, a highly immiscible system, by PS–PEO block copolymers alone. Others[10] have prepared oil-in-water microemulsions from block copolymers without cosurfactants.

Trace amounts of water are inevitably found in most organic solvents. Water strongly affects the structures formed by PS–PEO block copolymers beyond inducing microemulsions. We find unusually large structures in our driest solutions that disappear upon the addition of small amounts of water. Others[11-13] have observed large aggregates in solutions of PS–PEO diblock copolymers in selective solvents for polystyrene and have attributed their existence to the crystallizability of poly(ethylene oxide). We also believe the crystallizability of PEO is responsible for the large aggregates we find in dry cyclopentane; at higher water concentrations, water molecules dissolve the PEO chains reducing the driving force for formation of large aggregates.

Unusual structures have also been observed in ionic surfactant solutions with very low water content. Small rigid aggregates form in solutions of AOT (sodium 1,4-bis(2-ethylhexyl)sulfobutanedioate) in isooctane with water contents on the order of 25 ppm.[14] The heads of the surfactants are linked together by hydrogen bonds, with water acting as a "gluing" agent.[15,16] Unlike micelles at equilibrium, the aggregate size does not change as the temperature is varied from 0 to 50 °C. These structures are similar to large PEO–PS aggregates in that strong interactions between hydrophilic moieties promote the formation of structures not present at higher water contents.

0024-9297/90/2223-0745$02.50/0

Table I
Diblock Copolymer Characteristics

PEO/PS	mol wt[a]	M_w/M_n	wt % EO	N_{EO}	N_S
170/1730	187 500	1.10	4	170	1730
65/80	11 140	1.12	25.5	65	80

[a] Polymer Labs originally reported molecular weights of 184 000 and 9 800.

This study explores two features of poly(ethylene oxide), its compatibility with water and its crystallizability. Strong interactions between poly(ethylene oxide) blocks dominate the thermodynamic forces governing morphology at low water contents while water affects the size of spherical micelles at higher concentrations. Because of the presence of several polymeric species, our observations would not be as clear without size distributions from our dynamic light scattering experiments. We, therefore, include a brief discussion of our data analysis in the Experimental Section. We then present results and discussion addressing spherical micelles and large aggregates, in that order.

Experimental Section

1. Materials. Polystyrene–poly(ethylene oxide) diblock copolymers SE002 and SE003 were purchased from Polymer Laboratories Inc. They report molecular weights of 187 500 and 11 140 with corresponding ethylene oxide contents of 4 and 25.5 wt % based on GPC measurements of the polystyrene block and NMR experiments on the final block copolymer. They also estimate the polydispersity of the samples, M_w/M_n, from GPC measurements of the block copolymer. The copolymer characteristics are summarized in Table I. The samples will be identified henceforth by listing the degrees of polymerization of the ethylene oxide and styrene blocks, N_{EO}/N_S.

Glass-distilled deionized water was used in the purification of cyclopentane as well as in the preparation of samples. Cyclopentane was purchased from Eastman Kodak with a purity of 99%. It was treated by washing with concentrated sulfuric acid until the washings were colorless, followed by washing with water, a 10% sodium carbonate solution, and water again. The solvent was dried over sodium sulfate and then refluxed and distilled from a 50% sodium–paraffin dispersion with benzophenone.

2. Sample Preparation. Samples with polymer concentrations ranging from 20 to 12 000 ppm by weight were prepared either from dry solid-state copolymer or from dilutions of stock solutions. Water was added with a micropipet. Polymer concentrations were determined by using polystyrene UV absorption peaks at 262 and 269 nm. Light scattering samples were filtered through rinsed Millipore Fluoropore membrane filters with pore sizes of 0.2 or 0.5 μm. The light scattering cells were rinsed several times with filtered solvent before the sample was introduced in order to avoid dust contamination. Unchanging size distributions from dynamic light scattering revealed when the solutions had reached equilibrium. Use of a Burrell Model 75 wrist action shaker decreased the time needed to reach equilibrium, particularly necessary near saturation. A solution was considered saturated when excess water droplets were visible on the bottom of the scattering cell, after settling overnight.

Dry samples are difficult to prepare, even with cyclopentane distilled from sodium. Water is introduced to the samples during handling, particularly during the filtration process. In addition, some water accompanies the copolymer during dissolution. We found that by loosening the cell caps and placing the scattering cells in a desiccator, we could obtain samples with water content as low as 8 ppm. Since we determine our polymer concentrations spectrophotometrically, we can account for solvent lost along with water during this final drying step.

3. Water Content Measurement. We perform Karl Fischer titrations with an Aquastar C2000 coulometric titrator to determine water content. It is important to measure water content rather than estimate it from a mass balance because we are dealing with trace amounts. The titrator determines water concentration by measuring the absolute amount of water and dividing by the sample weight. The Aquastar C2000 titrator is capable of measuring as little as 10 μg of water. We are therefore limited by the size of our samples rather than the accuracy of the titrator. It is not a problem that the block copolymer is insoluble in the Karl Fischer solution; the solution is stirred vigorously, and the titration time is adjusted to avoid mass transfer limitations. Other investigators have shown that coulometric Karl Fischer titration can measure water electrostatically bound to insoluble proteins suspended in organic solvents.[17] Therefore, even water bound to ethylene oxide units should be detected by this method.

4. Dynamic Light Scattering. We use a Lexel Model 95 2-W argon ion laser to provide a light source with a wavelength of 514.5 nm. The incident beam is focused into a sample cell surrounded by index matching fluid and temperature controlled to ±0.05 °C by a water bath. All experiments were performed at 23 °C unless noted otherwise. The viscosity of cyclopentane, 0.432 cP, was measured with a Cannon-Ubbelohde capillary viscometer. An index of refraction of 1.4086 for cyclopentane at 514.5 nm and 23 °C was obtained from the literature by interpolations for wavelength and temperature dependence.[18] We routinely collect homodyne dynamic light scattering data at laboratory scattering angles of 30°, 60°, 90°, and 150° using a Brookhaven Instruments BI-200 goniometer. Refraction corrections for square cells give effective scattering angles of 31.1°, 58.9°, 90°, and 148.9°, respectively. Digital signals from the goniometer are processed on a Brookhaven Instruments BI2030 136-channel correlator.

Dynamic Light Scattering Data Analysis

Dynamic light scattering is becoming a popular technique for investigating polymeric micellar solutions. Early studies have used single exponential or cumulant fits in their data analysis.[7,9,19–22] The first method is valid for sizing monodisperse particles while the second method gives information about the polydispersity of the particles in addition to an average particle size. These data analysis techniques are appropriate when the single chain size or scattering signal is too small to be detected; however, single chains in polymeric micellar solutions are often large enough to be detected by light scattering. Zhou and Chu attempted, but were not able, to distinguish single chains from micelles because of the relatively large polydispersity of the commercial Pluronic block copolymers used in their study.[23,24] Single chains and micelles are easily resolved in the system reported in this paper by using a constrained regularization technique developed by Provencher.[25] We find that our dynamic light scattering results are much more enlightening when we monitor the sizes of the individual species in solution rather than interpret average size information.

A second-order temporal correlation function is generated from the digital photocounts

$$g^{(2)}(\tau) = \frac{\langle I(0)I(\tau)\rangle}{\langle I(0)\rangle^2} \quad (1)$$

where, in the numerator, the angular brackets denote the time average of a product of intensities separated by a delay time, τ. The correlation function is normalized by the square of the base line, $\langle I(0)\rangle$, obtained either from delay channels (the measured base line) or from calculating the average intensity (the calculated base line). The choice of base line is insignificant for samples with low levels of dust. Base-line agreement was generally within 0.1% for the measurements reported in this investigation indicating the samples were clean.

For scattered light following Gaussian statistics, the second-order correlation function is related to the first-

order correlation function by[26]

$$g^{(2)}(\tau) = 1 + f(A)|g^{(1)}(\tau)|^2 \quad (2)$$

where $f(A)$ depends on the sampling interval and scattering geometry and is usually determined by a fit to experimental data. Theoretical forms of the first-order correlation function can be derived for various physical processes. For a dilute solution of relatively small monodisperse particles it is directly related to translational diffusion

$$g^{(1)}(\tau) = \exp(-q^2 D\tau) \quad (3)$$

Here the decay rate contains the translational diffusion coefficient of the particles, D, and the square of the magnitude of the scattering vector, $q = (4\pi/\lambda)\sin(\theta/2)$, where λ is the wavelength of light in the medium and θ is the scattering angle. If the particles are noninteracting spheres, the Stokes–Einstein relation

$$D = kT/6\pi\eta R_h \quad (4)$$

provides an expression for the hydrodynamic radius, R_h, where k is Boltzmann's constant, T the absolute temperature, and η the viscosity of the solvent.

In the absence of detectable internal or rotational motions, the first-order correlation function for a dilute solution of polydisperse particles comprises a sum over all possible hydrodynamic sizes

$$g^{(1)} = \int_0^\infty F(R_h) \exp\left\{-\left[\left(\frac{q^2kT}{6\pi\eta}\right)R_h^{-1}\tau\right]\right\} dR_h \quad (5)$$

where $F(R_h)\,dR_h$ represents the fraction of the total integrated intensity scattered by particles with effective hydrodynamic radii between R_h and $R_h + dR_h$. The intensity distribution, $F(R_h)$, can be converted to a number distribution, $\rho(R_h)$ via[27]

$$F(R_h) = B\alpha(R_h)^2 S(R_h)\rho(R_h) \quad (6)$$

where B is a normalization factor, $\alpha(R_h)$ is the polarizability of a particle with hydrodynamic size R_h, and $S(R_h)$ is the particle form factor (also dependent on the scattering vector length, q).

We use three techniques to obtain size distribution information from the measured time correlation functions. The Brookhaven correlator software includes a single exponential fit and a second-order cumulant fit.[28] A comparison of the goodness of fit obtained from these two methods reveals whether the autocorrelation function better represents a solution of monodisperse particles or a solution with a more complicated particle size distribution. It is particularly helpful in the latter case to evaluate the data in more detail by inverting the Laplace transform given in (5) to obtain an explicit size distribution. Several inversion methods have been proposed with varying success.[29–35] Difficulty in determing the true size distribution arises because an unbounded number of solutions will fit data within experimental noise. Because these distributions can have arbitrarily large deviations from each other and because often a highly oscillatory distribution will best fit the data, chances are small that unconstrained inversion of the autocorrelation function will yield a physically meaningful size distribution.

To circumvent the ill-posed nature of this inversion, we use a procedure developoed by Provencher[36–38] to find the smoothest nonnegative size distribution consistent with the data. The program, called CONTIN, for continuous distribution, is written in FORTRAN. We run CONTIN on a Sun 3/260 with a floating point accelerator.

In general, CONTIN inverts noisy linear operator equations, of which the Laplace transform is a special case. Combining 2 and 5 yields a Laplace transform relationship between the measured second-order correlation function, $g^{(2)}(\tau)$, and the intensity distribution, $F(R_h)$

$$(g^{(2)}(\tau)-1)^{1/2} = \int_0^\infty F(R_h) \exp\left\{-\left[\left(\frac{q^2kT}{6\pi\eta}\right)R_h^{-1}\tau\right]\right\} dR_h + \Delta_2 \quad (7)$$

where Δ_2 allows for a possible constant background contribution to $g^{(1)}(\tau)$ due to scattering from dust.[25] A quadratic programming algorithm finds a unique solution minimizing an objective function consisting of the weighted sum of squared residuals plus a smoothing term penalizing solutions with increased amounts of curvature. The optimum amount of smoothing is large enough to smooth out spurious oscillations without distorting the true features of the solution. Systematic choice of the smoothing parameter will be discussed below. The solution is further stabilized by constraining both the size distribution and the dust term to be nonnegative.

CONTIN is more robust to artifacts created by noise than most other data analysis techniques because of the smoothing parameter. The output includes several solutions obtained with varying amounts of smoothing along with their residual plots. CONTIN software includes a statistical method to automatically choose the amount of smoothing based on a Fisher test. A "probability one to reject" is calculated for each solution comparing its variance with the variance of the unsmoothed solution, with values increasing monotonically (from 0 to 1) with increased smoothing. Provencher suggests choosing the solution with a "probability one to reject" of 0.5, so that the increase in the objective function of the smoothed solution compared to that of the unsmoothed solution could be attributed 50% of the time to chance alone and 50% to oversmoothing. An alternative method of choosing the smoothing parameter has been proposed by Bott using threshold statistics.[39] Here, the smoothest solution is chosen such that the Laplace transform of the difference between the smoothed and unsmoothed solutions is undetectable within the bounds of the noise in the data. Limited tests[39] comparing these two statistical approaches show that a "probability one to reject" of 0.4 in the Provencher method corresponds to the optimum smoothing from the Bott method. Considering that Bott made fewer and more appropriate assumptions, it may be preferable to use less smoothing than recommended by Provencher when analyzing dynamic light scattering data.

Several groups have tested CONTIN with experimental data from solutions with well-characterized monomodal and bimodal distributions and with data simulated with and without noise.[25,27,34,36,40,41] A difference of a factor of 2 in hydrodynamic radius appears to be close to the resolution limit of the technique. Bimodal distributions with sizes separated by a factor of 4 are easily resolved as long as the intensity fraction of the smaller peak exceeds approximately 5%.[27]

Most solutions in this study contain two if not three distinct species. Dynamic light scattering is well suited for studying these systems because the relaxation times corresponding to the translational motion of the different species are indeed separated by approximately a factor of 4. Since the effect of oversmoothing is more significant for multimodal distributions, we systematically choose solutions with a "probability one to reject" of 0.2, less smoothing than suggested by Provencher. We routinely collect several data sets (on the order of 10) for each sample at multiple angles. If the residual error

between the measured and proposed autocorrelation functions is not random, the chosen solution from that data set is deemed unacceptable. Error bars with the distribution indicate whether features of the solution are uncertain. Comparison of several solutions at each angle helps us distinguish physical from unphysical peaks. Measurements at several angles further aids our interpretation of the data, providing information about the reliability of the distributions as well as information about the polydispersity of relatively large species.

Occasionally a small peak is observed at the lower edge of the size distribution with error bars larger than the magnitude of the peak. It usually represents less than 1% of the total scattering intensity, unlike spurious peaks from other analysis techniques that are not stabilized by a smoothing term. This same small peak has been observed infrequently by Sorlie and Pecora while using CONTIN to analyze both experimental and simulated data with added Gaussian noise.[41] They note that the presence of the small peak did not appreciably alter the positions of the other peaks in the simulated data. Since an anomalous first autocorrelation channel can cause a small peak at the lower end of the size distribution, we discard the first point as done in the Sorlie and Pecora study. CONTIN, in general, does not overestimate the number of relaxation responsible for a given correlation function. All other resolved peaks in this study represent the translational motion of identifiable polymeric species.

Dust is always avoided in the preparation of light scattering samples since the results are very sensitive to low concentrations of large particles. CONTIN can tolerate low levels of dust with its allowance for a constant background scattering contribution, working at dust levels where the method of cumulants fails. Tests of CONTIN suggest that a maximum safe level of dust occurs when the normalized dust term of eq 7, Δ_2, is approximately 0.05.[25] Dust was not a problem in this study; any distributions with nonzero dust terms were discarded.

Results

1. **Micellar Solutions.** Typical size distributions obtained from dynamic light scattering are illustrated in Figure 1, where, for each block copolymer, we demonstrate the size distribution before and after the addition of water. The large difference in hydrodynamic size enables us to identify both single chains and micelles. In a solution of the larger polymer, PEO/PS = 170/1730, with a polymer and water content of 1500 and 28 ppm, respectively, we find micelles with a hydrodynamic radius of 34 nm. The single chain hydrodynamic radius of 8 nm compares well with an estimate of 10 nm from the intrinsic viscosity of equivalent polystyrene chains in near Θ solvents.[42] The solution contains 92% micelles based on an intensity distribution. We present intensity distributions to avoid making assumptions regarding particle shape; weight or number distributions would require models for the particle polarizabilities and form factors shown in eq 6. Since intensity distributions heavily weight the large scatterers, if we assume the single chains and micelles are homogeneous polystyrene spheres, we find the same solution contains 15% micelles by weight or only 0.3% by number.

It is appropriate to characterize a peak in a CONTIN size distribution by its mean R_h and intensity fraction rather than by its shape. A better measure of polydispersity involves a comparison of micelle size as a function of angle. The Rayleigh–Debye form factor for a homogeneous polystyrene sphere with a radius of 34 nm increases from 0.87 to 0.98 as the scattering angle decreases from 90° to 30°.

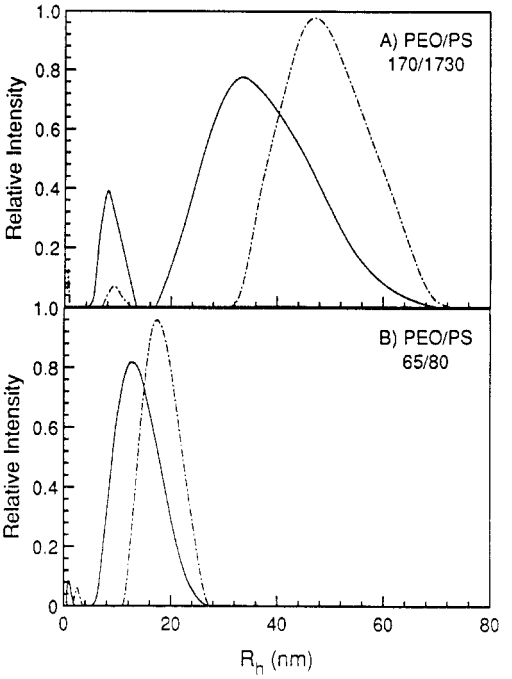

Figure 1. Effect of water on intensity weighted size distributions for (A) 1500 ppm 170/1730 copolymer with (—) 28 ppm water and (- · -) 98 ppm water and (B) 5800 ppm 65/80 copolymer with (—) 155 ppm water and (- · -) 1030 ppm water. The peaks represent single chains and spherical micelles in ascending order.

If the micelles are polydisperse, the micelle hydrodynamic radius would appear larger at lower angles due to the angular dependence of the form factor. Since the micelle R_h measured at 30°, 60°, and 90° agree within experimental error, we conclude that the micelles are relatively monodisperse.

Water plays an important role in micellization since it is a selective solvent for poly(ethylene oxide), the block in the micellar core. The effect of water on micellar structure is evident in Figure 1; the micelle hydrodynamic radius increases from 34 to 48 nm as the water content is increased from 28 to 98 ppm in a 1500 ppm solution of the 170/1730 block copolymer. Concurrently, the intensity fraction of micelles increases from 92% to greater than 99%. In addition to swelling the micellar core and probably increasing the micelle aggregation number, water promotes micellization from a larger percentage of the block copolymer.

We illustrate the dependence of micelle hydrodynamic radius on water and polymer concentrations in Figure 2. We measured micelle R_h between additions of water to solutions of three polymer concentrations. The error bars represent variations of one standard deviation for several water content and (6–10) light scattering measurements. Addition of less than 100 ppm of water can increase the micelle size by as much 40%, with most of the size change occurring below 87 ppm, the saturation point of cyclopentane at 23 °C. Further analysis of the partitioning of water in the micelles is precluded by our inability to distinguish water associated with micelles from that in cyclopentane.

The saturated micelle size appears constant for the three polymer concentrations shown in Figure 2. The variation in saturated micelle R_h values of 47.1, 46.8, and 48.1 nm corresponding to polymer concentrations of 9500, 4500, and 1500 ppm, respectively, is not significant. However, the saturated micelle hydrodynamic radius does not remain constant over the entire polymer concentration range inves-

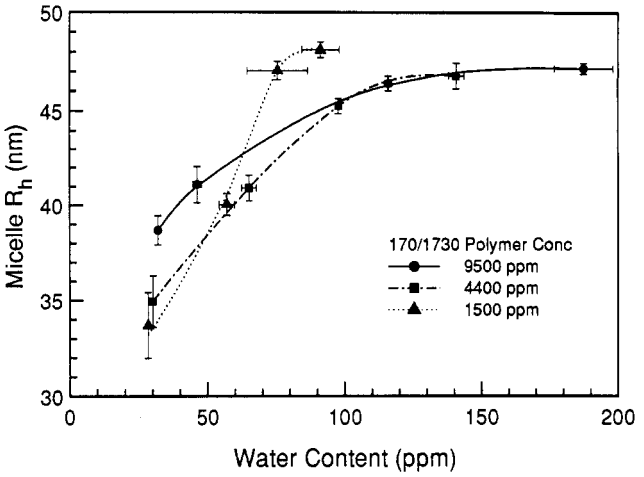

Figure 2. Micelle hydrodynamic radius as a function of water content at 170/1730 polymer concentrations of (●) 9500 ppm, (—) 4400 ppm, and (▲) 1500 ppm.

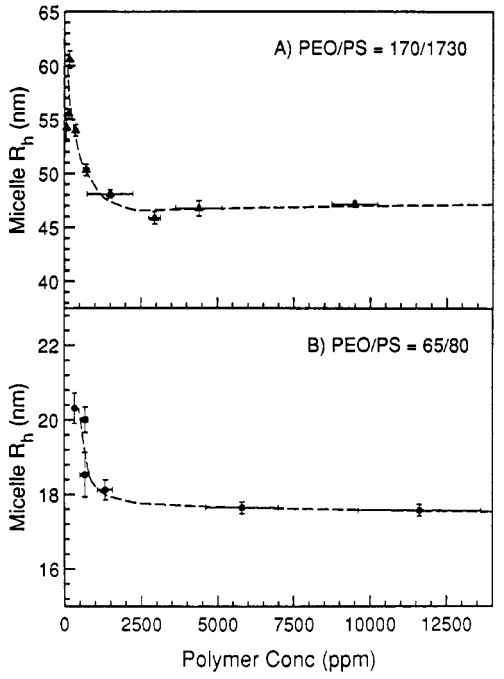

Figure 3. Saturated micelle hydrodynamic radius as a function of (A) 170/1730 and (B) 65/80 polymer concentrations, indicating a change in micelle structure at low water contents.

tigated. At very low polymer concentrations, Figure 3 displays an increase in hydrodynamic size as much as 30% from the constant value of 47 nm in the more concentrated solutions. Note that all concentrations in this study are dilute; interactions between micelles do not appear to affect the translational diffusion of micelles in any of the samples investigated. We believe the increase in saturated micele R_h at very low polymer concentration indicates a change in the micellar structure.

This study also focuses on the sensitivity of the critical micelle concentration, cmc to trace amounts of impurities selective for the insoluble block. The critical micelle concentration is defined as the limit below which virtually no micelles are detected and above which almost all additional block copolymer goes into the micellar phase.[43] The cmc for polystyrene–poly(ethylene oxide) block copolymers in dry cyclopentane would pertain to the onset of large aggregate formation (discussed below). At higher water contents, spherical micelles are preferred over large aggregates. Although it is not clear whether the concept of a cmc is applicable to systems of two immiscible solvents, we are interested in the effect of water content on the transition from single chains to swollen micelles. While we see only single chains at water and 170/1730 copolymer concentrations of 21.5 and 22 ppm, respectively, the same solution saturated with water contains greater than 99% micelles. If a critical micelle concentration exists for saturated solutions of the 170/1730 copolymer, it is below the resolution limits of our dynamic light scattering experiment. Yet, since we observe relatively dry solutions without micelles, it is clear that the addition of water lowers the concentration where micelles appear. This effect of water on the "cmc" provides further proof that the addition of water favors spherical micelle formation.

The smaller block copolymer, PEO/PS = 65/80, exhibits trends similar to the 170/1730 sample as polymer and water concentrations are varied. Figure 1B contains representative intensity weighted size distributions for this sample. Recall that in addition to having an order of magnitude lower molecular weight than the 170/1730 sample, the smaller block copolymer contains a much higher percentage of poly(ethylene oxide), the insoluble block. We observe micelles with a hydrodynamic radius of 13 nm in a solution of 5800 ppm of polymer and 155 ppm of water, while R_h expands to 18 nm at 1030 ppm of water. We expect the single chain to have a hydrodynamic radius on the order of 2 nm, based on intrinsic viscosity estimates. The 65/80 single chains are difficult to measure because their diffusional relaxation time is close to the peak related to experimental noise described above. In samples with relatively low water and polymer concentrations, we can unambiguously resolve single chains of the 65/80 block copolymer with an R_h of approximately 2 nm; its identification is less certain when its contribution to the total scattering intensity is small.

Figure 3 displays the saturated micelle size as the polymer concentration is varied. We again observe an increase in saturated micelle R_h at very low polymer concentrations, changing by 20% over the polymer concentration range investigated for the 65/80 sample. Micelles dominated the size distributions of all of the saturated solutions prepared down to a polymer concentration of 330 ppm. Thus, if a concentration analogous to the cmc exists for saturated solutions of the 65/80 sample, it is below 330 ppm.

Although micelles formed by each of the two block copolymers are similar in many respects, we find the 65/80 sample is more effective in dispersing water in cyclopentane. When the water content of saturated solutions versus PEO content is plotted in Figure 4, we see a large difference in dispersion capabilities between the two block copolymers. Here the error bars for water content represent one standard deviation from several Karl Fischer titrations, while the error bars for PEO content represent the uncertainty in solution concentrations. Converting the slopes to mole ratios yields 1.8 mol of water molecules/mol of EO repeat units for the 65/80 sample while only 0.7 mol of water/mol of EO for the 170/1730 sample, indicating that micelles composed of the 65/80 block copolymer can accommodate approximately twice as much water as micelles from the 170/1730 copolymer per EO repeat unit. In light of the change in saturated micelle structure at low polymer concentrations illustrated in Figure 3, we note that the micellar size for the 65/80 and 170/1730 samples increases below 250 and 40 ppm of PEO, respectively. Combining these results suggests that, while the increase in saturated micelle size

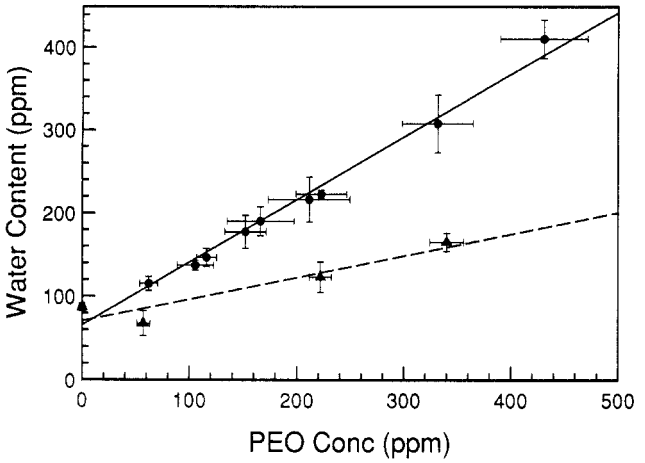

Figure 4. Dispersed water as a function of poly(ethylene oxide) concentration. The (●) 65/80 and (▲) 170/1730 block copolymers solubilize approximately 1.8 and 0.7 water molecules per EO repeat unit, respectively.

may involve an aggregation number change, the relative water to EO content ratio remains constant within experimental error.

2. Solutions with Large Aggregates. Relatively dry solutions of these block copolymers in cyclopentane contain structures too large to be spherical micelles. Figure 5 displays intensity weighted size distributions for solutions of 1300 ppm of 65/80 block copolymer with varying water content. At 34 ppm of water, we find large aggregates with an average effective hydrodynamic radius of 63 nm as well as single chains and micelles. Addition of water promotes formation of micelles from both single chains and large aggregates, with the micelle intensity fraction increasing from 0.03 to 0.12 and 0.99 as the water content is increased. The large aggregates coexist with relatively unswollen micelles, as evidenced by the micelle R_h value of 10.1 ± 0.4 nm in the solution with 57 ppm of water in Figure 5.

The large aggregates appear stable for periods longer than a month. Furthermore, their presence in relatively dry solutions is very reproducible. Figure 6 illustrates the structures present as a function of water and 65/80 copolymer concentrations. Rather than finding a transition from micelles to large aggregates, we observe a large window of polymer and water concentrations where they coexist. Single chains are present in all solutions, although their contribution to the correlation function is sometimes too small to resolve.

We prepared most samples from dry solid-state copolymer and purified solvent and measured size distributions between additions of water. When large aggregates are present, their average effective R_h ranges from 40 to 110 nm. As the scattering angle is decreased from 90° to 30°, the aggregate effective R_h increases by as much as 15 nm, suggesting that they are more polydisperse than the spherical micelles reported above. Samples with large aggregates may also be prepared by drying out solutions containing only micelles using the procedure described in the Experimental Section; however, solutions prepared in this manner have even larger aggregates, with R_h on the order of 300–400 nm.

To address the question of reversibility, we investigated the effect of changing temperature with a sealed sample of large aggregates. The sample was heated to 30 and 40 °C and cooled back down to 23 °C without substantial changes in the size distribution of the structures in solution. When the sealed sample is heated to

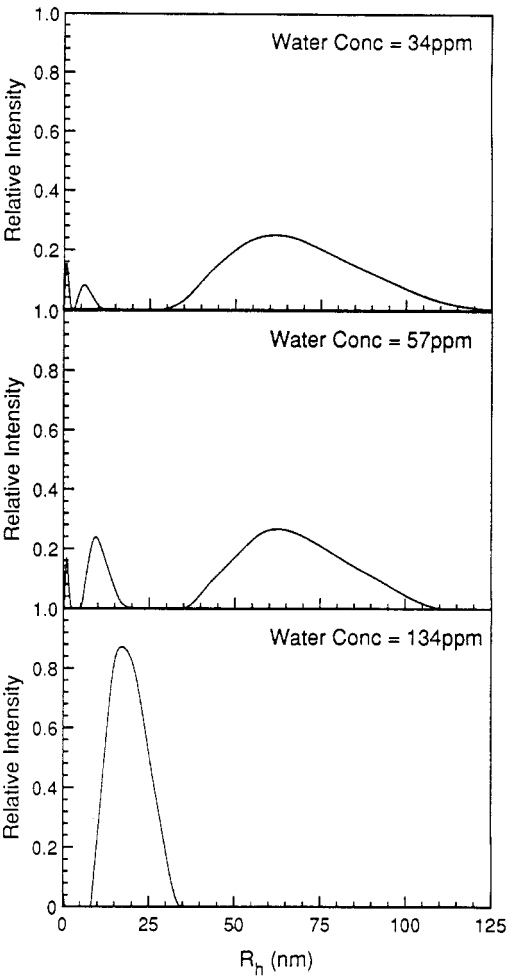

Figure 5. Effect of water on the intensity weighted size distributions in solutions of 1300 ppm 65/80 polymer measured at 90°. The peaks represent single chains, spherical micelles, and large aggregates in ascending order. Large aggregates are not present in solutions with high water contents.

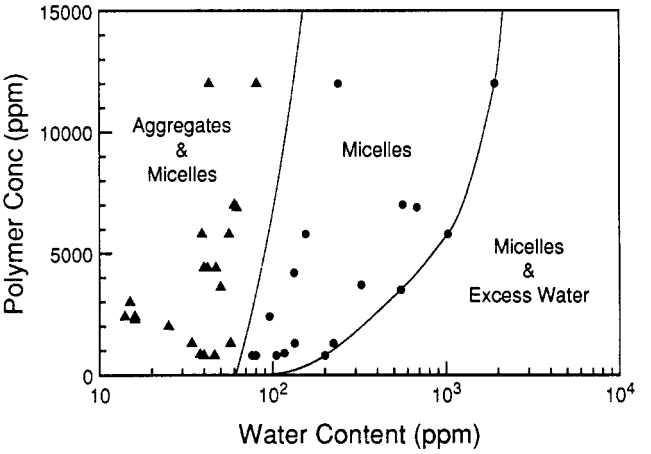

Figure 6. Phase diagram for the 65/80 block copolymer at 23 °C. All solutions contain single chains in addition to large aggregates and/or spherical micelles.

68 °C, however, above the melting temperature of poly(ethylene oxide),[44,45] the solution appeared to contain only single chains. Subsequent cooling back to 23 °C resulted in the formation of very large aggregates over a period of 24–48 hours. Eventually, the aggregates became so big that they settled out of solution and were visible to the naked eye. These temperature experiments reveal that solutions containing aggregates may be very slow to

equlibrate, making it difficult to ascertain their equilibrium structure. A solution with enough water so as only to contain micelles and single chains was also sealed and subjected to similar temperature changes with no observed changes in size distribution.

Solutions with large aggregates have also been prepared from the PEO/PS = 170/1730 sample. Large structures are formed in these solutions when the water content is below approximattely 20 ppm. Generally, solutions made from dry solid-state 170/1730 copolymer and purified solvent need to be dried further in order to reach water concentrations where large aggregates exist.

Discussion

1. Micellar Solutions. Two polymeric species, micelles and single chains, were resolved in solutions of the 170/1730 and 65/80 block copolymers with water contents greater than approximately 25 and 70 ppm, respectively. The narrow size distribution of the micelles suggests that they are spherical, as opposed to inherently polydisperse wormlike micelles.[46,47] The micelle size relative to that of a single chain is also consistent with the inference of sphericity. From our water content measurements of saturated micelles, we find that the cores contain, at most, two water molecules per ethylene oxide repeat unit. Because the PEO block comprises only 10 mol % of the 170/1730 block copolymer, the large increase (40%) in micelle hydrodynamic size exhibited in Figure 2 as water content is increased would not be accomplished if the micelle aggregation number did not increase also. Increases in aggregation numbers have been observed as water content is increased in water in oil microemulsions stabilized by AOT.[48]

In order to study a system with a well-defined partitioning of water, we investigate the dependence of the water-saturated micelle size on copolymer concentration. We observe an abrupt increase in micelle R_h at very low polymer concentrations, similar to that observed for a triblock copolymer in a single solvent.[49] This contrasts with the concentration dependence of the translational diffusion coefficient due to interparticle interactions, approximated by

$$D = D_0(1 + k_d C) \tag{8}$$

where D_0 is the z-average diffusion coefficient at infinite dilution and k_d is the diffusion second virial coefficient. Since D is inversely related to R_h, Figure 3 illustrates that we do not measure a linear relationship between the saturated micelle diffusion coefficient and concentration. In particular, the unchanging micelle hydrodynamic size in the high concentration end of the concentration range suggests that particle interactions are not significant.

Monitoring the time dependence of the saturated micelle size after dilution provides evidence that micelles do indeed undergo a structural change at low polymer concentration. We diluted a solution with a 170/1730 concentration of 2950 to 165 ppm and observed a change in R_h from 47.8 ± 0.5 nm to 52.2, 57.0, and 60.6 ± 0.8 nm when we collected correlation functions 1, 3, and 20 h after dilution, respectively. The slow approach to equilibrium implies a rearrangement of the saturated micelle structure at low copolymer concentrations.

A number of similarities can be found between the structural behavior of our nonionic block copolymers and AOT dispersed in hydrocarbons. An increase in swollen micelle radius at high dilution has been observed with X-ray scattering from solutions of AOT in decane with a constant water-to-AOT molar ratio of 30.[50] They predict an increase in radius at very low AOT concentrations as the fraction of surfactant dispersed in the continuous phase increases, based on a constant interfacial area per surfactant molecule. In a higher surfactant concentration range, a slight increase in micelle R_h with increasing AOT concentration has been measured with dynamic light scattering for AOT in isooctane with similar water-to-AOT ratios.[14] They attribute the small change in R_h to a partitioning of water from micelles into the newly added continuous phase and would presumably observe a constant micelle hydrodynamic radius if the amount of water in the micellar phase did not change upon dilution. Our saturated polymeric micelles resemble both studies of surfactant micelles described above. We find larger swollen micelles at very low copolymer concentrations. We measure an unchanging saturated micelle size at higher concentrations; water partitioning does not affect our comparison because the background water concentration is constant. However, considering AOT is an ionic surfactant molecule, the same phenomena may not be responsible for the similarity in observations.

In the spirit of the theory of surfactant self-assembly developed by Israelachvili, Mitchell, and Ninham,[47,51] we use geometric arguments to rationalize the difference in dispersion capabilities between the two copolymer samples. The microemulsion size is influenced by the optimal interfacial area per surfactant molecule. This, in turn, is affected by the composition of the block copolymer as well as the extent to which each block is swollen by its respective selective solvent. Because the polystyrene block in the micelle corona comprises 91 mol % of the 170/1730 sample, this block copolymer will prefer a cone- or wedge-shaped conformation at the water–oil interface. On the other hand, the more symmetric 65/80 sample can adapt more easily to an interface with less curvature and can thus disperse more water.

2. Solutions with Large Aggregates. We repeatedly observed unusual aggregates in solutions of the 65/80 and 170/1730 block copolymers with water contents below 70 and 25 ppm, respectively. Geomeric arguments preclude their identification as spherical micelles because of their size relative to that of a single chain. With effective hydrodynamic diameters larger than 150 nm, internal flexing of wormlike micelles should be observed in the appearance of dynamic form factors at high scattering angles.[27] In search of an additional decay time corresponding to internal motions, we analyzed correlation functions from a scattering angle of 150° with DISCRETE[35] as well as CONTIN. DISCRETE, also written by Provencher, fits the data with a sum of up to five exponentials. Neither analysis technique distinguished a fourth decay time, suggesting the large aggregates are not wormlike micelles.

Unusually large structures, referred to as anomalous micelles, have been observed by several investigators at the onset of micellization when changing temperature or mixed-solvent composition.[19,21,52-54] In a few of these studies, the anomalous micelles have been clearly identified as wormlike micelles.[46,55-57] Tuzar et al. have demonstrated that the presence of insoluble homopolymer can be responsible for the presence of anomalous micelles.[58] Recently, Zhou and Chu have shown that the presence of a small amount of copolymer with a high content of the insoluble block can also cause anomalous micellization as long as the phase separation of the "impurity" occurs before the onset of micellization of the major component.[24] The large aggregates observed in this study are not another example of anomalous micelles. The PEO–

PS aggregates form over a wide range of copolymer concentrations, not just in the vicinity of the cmc. Furthermore, rather than being induced by the presence of an impurity, the large aggregates break up upon the addition of water.

The existence of large aggregates is clearly related to water content (see Figure 6). We believe the driving force for forming these large structures involves the crystalizability of the poly(ethylene oxide) insoluble block. Strong interactions among poly(ethylene oxide) blocks may promote a more ordered insoluble domain with less curvature. Water acting as a diluent may diminish these interactions and reduce the crystallinity. Identification of these large aggregates as vesicles or lamellae would be consistent with these arguments, although we have no firm evidence at this time.

Franta[12] has performed static light scattering, electric birefringence, and dielectric constant measurements on PS–PEO diblock copolymers in ethylbenzene, a selective solvent for polystyrene, and has observed big anisotropic aggregates. Big aggregates were not observed in methanol, a selective solvent for poly(ethylene oxide).[11] A lamellar structure was proposed for the big aggregates, similar to that seen for the same system at elevated concentrations.[59] Lamellar structures with crystallizable domains have been seen with an optical microscope in dilute solutions of PS–PEO diblock copolymers in ethylbenzene, xylene, and isoamyl acetate.[13]

Some interesting analogies can be made between structures formed by PEO–PS diblock copolymers in solution and in blends. Small-angle X-ray scattering and differential scanning calorimetry measurements reveal that, whenever crystallized structure is observed in PEO–PS blends, the structure is always lamellar.[45,59,60] Unlike crystallizable homopolymers, where chain folding is metastable, the crystallizable block adapts to the thermodynamic forces of the crystalline and amorphous domains by folding into an equilibrium thickness.[61] Increasing the polystyrene block length or swelling the polystyrene block results in a thinner PEO layer with more chain folds. The crystallized PEO structure disappears upon addition of more than 0.66 mol of nitromethane and acetic acid, selective solvents for PEO, per mole of EO repeat units in a blend of PEO/PS = 125/85. At these solvent concentrations or above the melting point, the structure with melted PEO blocks is governed by the copolymer composition, as seen with other amorphous block copolymers,[62,63] where hexagonal and reversed hexagonal structures are formed in addition to lamellar structures with amorphous domains. A recent equilibrium theory[64] for block copolymers with a crystallizable block is in general agreement with these observations.

We have observed the formation of large aggregates with both block copolymers, even though the composition of the 170/1730 sample is highly asymmetric. The disappearance of the large aggregates of 170/1730 at lower water contents than those of 65/80 can be attributed to the greater imbalance in composition. Current studies in our laboratory are focused on investigating the structure of these large polymeric aggregates.

Conclusions

We have demonstrated the benefits of obtaining size distributions from dynamic light scattering rather than an average size, especially when more than one species contributes significantly to the autocorrelation function. Data from solutions with large aggregates would have been particularly difficult to interpret from an average diffusion coefficient.

We find the structures formed in dilute solutions of polystyrene–poly(ethylene oxide) in cyclopentane are very sensitive to trace amounts of water. Large aggregates coexist with spherical micelles at very low water contents. Their existence appears to depend on the crystallizability of the insoluble block and would, therefore, not be expected for all block copolymers in hydrocarbons with low water content. The addition of water breaks up the large aggregates, resulting in a solution of monodisperse spherical micelles and single chains. In solutions with only single chains, an increase in water content lowers the concentration at which micelles are first detected. Water not only increases the fraction of block copolymers participating in micelles but also increases the micelle hydrodynamic radius. We find that, of our two block copolymers, the more symmetric copolymer is more effective at dispersing water in cyclopentane. Furthermore, saturated micelles from both block copolymers exhibit a dramatic increase in hydrodynamic size at high dilution.

Acknowledgment. This work has been partially supported by the Center for Materials Research at Stanford University under the NSF-MRL program and the du Pont Marshall Laboratory. K.A.C. appreciates support from the Eastman Kodak Co. and AT&T Bell Laboratories. We thank Thomas Bender, Adam Cantor, Robert Pecora, and Susan Sorlie for their help in establishing our dynamic light scattering capabilities and S. W. Provencher for use of his program, CONTIN. We also gratefully acknowledge useful discussions with Frans Leermakers and Mark Munch.

References and Notes

(1) Tuzar, Z.; Kratochvil, P. *Adv. Colloid Interface Sci.* **1976**, *6*, 201.
(2) Riess, G.; Bahadur, P.; Hurtrez, G. *Encyclopedia of Polymer Science and Engineering* Wiley: New York, 1985; Vol. 2, p 324.
(3) Gast, A. P. *NATO ASI Proc.* **1988**, in press.
(4) Hager, B. L.; Berry, G. C.; Tsai, H.-H. *J. Polym. Sci., Polym. Phys. Ed.* **1987**, *25*, 387.
(5) Riess, G.; Nervo, J.; Rogez, D. *Polym. Eng. Sci.* **1977**, *17*, 634.
(6) Marie, P.; Duplessix, R.; Gallot, Y.; Picot, C. *Macromolecules* **1979**, *12*, 1180.
(7) Boutillier, J.; Candau, F. *Colloid Polym. Sci.* **1979**, *257*, 46.
(8) Ballet, F.; Candau, F. *J. Polym. Sci., Polym. Chem. Ed.* **1983**, *21*, 155.
(9) Barker, M. C.; Vincent, B. *Colloids Surf.* **1984**, *8*, 297.
(10) Nagarajan, R.; Barry, M.; Ruckenstein, E. *Langmuir* **1986**, *2*, 210.
(11) Gallot, Y.; Franta, E.; Rempp, P.; Benoit, H. *J. Polym. Sci., Part C* **1964**, *4*, 473.
(12) Franta, E. *J. Chim. Phys.* **1966**, *63*, 595.
(13) Lotz, B.; Kovacs, A. J. *Kolloid-Z.* **1966**, *209*, 97.
(14) Zulauf, M.; Eicke, H.-F. *J. Phys. Chem.* **1979**, *83*, 480.
(15) Zundel, G. *Hydration and Intermolecular Interaction*; Academic Press: New York, 1969.
(16) Eicke, H.-F.; Christen, H. *Helv. Chim. Acta* **1978**, *61*, 2258.
(17) Zaks, A.; Klibanov, A. M. *J. Biol. Chem.* **1988**, *263*, 8017.
(18) Huglin, M. B. *Light Scattering From Polymer Solutions*; Academic Press: London, 1972.
(19) Mandema, W.; Emeis, C. A.; Zeldenrust, H. *Makromol. Chem.* **1979**, *180*, 1521. Mandema, W.; Emeis, C. A.; Zeldenrust, H. *Makromol. Chem.* **1979**, *180*, 2163.
(20) Oranli, L.; Bahadur, P.; Riess, G. *Can. J. Chem.* **1985**, *63*, 2691.
(21) Duval, M.; Picot, C. *Polymer* **1987**, *28*, 798.
(22) Tang, W. T.; Hadziioannou, G.; Cotts, P. M.; Smith, B. A.; Frank, C. W. *Polym. Prepr. (Am. Chem. Soc., Div. Polym. Chem.)* **1986**, *27*, 107.
(23) Zhou, Z.; Chu, B. *J. Colloid Interface Sci* **1988**, *126*, 171.
(24) Zhou, Z.; Chu, B. *Macromolecules* **1988**, *21*, 2548.
(25) Provencher, S. W.; Hendrix, J.; DeMaeyer, L.; Paulussen, N. *J. Chem. Phys.* **1978**, *69*, 4273.
(26) Berne, B. J.; Pecora, R. *Dynamic Light Scattering*; Wiley: New York, 1976.
(27) Flamberg, A.; Pecora, R. *J. Phys. Chem.* **1984**, *88*, 3026.

(28) Koppel, D. E. *J. Chem. Phys.* **1972**, *57*, 4814.
(29) Ostrowsky, N.; Sornette, D.; Parker, P.; Pike, E. R. *Opt. Acta* **1981**, *28*, 1059.
(30) Chu, B.; Gulari, E.; Gulari, E. *Phys. Scr.* **1979**, *19*, 476.
(31) Livesay, A. K.; Licinio, P.; Delaye, M. *J. Chem. Phys.* **1986**, *84*, 5102.
(32) Morrison, I. D.; Grabowski, E. F. *Langmuir* **1985**, *1*, 496.
(33) Cummins, P. G.; Staples, E. J. *Langmuir* **1987**, *3*, 1109.
(34) Stock, R. S.; Ray, W. H. *J. Polym. Sci., Polym. Phys. Ed.* **1985**, *23*, 1393.
(35) Provencher, S. W. *J. Chem. Phys.* **1976**, *64*, 2772.
(36) Provencher, S. W. *Makromol. Chem.* **1979**, *180*, 201.
(37) Provencher, S. W. *Comput. Phys. Commun.* **1982**, *27*, 213.
(38) Dr. S. W. Provencher generously provides copies of his computer program CONTIN for nonprofit institutions. His address is: S. W. Provencher, Max-Planck-Institut Fuer Biophysikalische Chemie, Postfach 2841, D-3400 Goettingen, Federal Republic of Germany. It can also be obtained using an order in any issue of *Comput. Phys. Commun.*
(39) Bott, S. E. Ph.D. Thesis, Stanford University, Stanford, CA, 1984.
(40) Bott, S. In *Measurement of Suspended Particles by Quasi-Elastic Light Scattering*; Dahneke, B. E., Ed.; Wiley: New York, 1983; p 129.
(41) Sorlie, S. S.; Pecora, R. *Macromolecules* **1988**, *21*, 1437.
(42) Brandrup, J.; Immergut, E. H. *Polymer Handbook*; Wiley: New York, 1975.
(43) Mysels, K. J.; Mujerjee, P. *Pure Appl. Chem.* **1979**, *51*, 1083.
(44) Odian, G. Principles of Polymerization; Wiley: New York, 1981.
(45) Gervais, M.; Gallot, B. *Makromol. Chem.* **1973**, *171*, 157.
(46) Canham, P. A.; Lally, T. P.; Price, C.; Stubbersfield, R. B. *J. Chem. Soc., Faraday Trans. 1* **1980**, *76*, 1857.
(47) Israelachvili, J. N.; Mitchell, D. J.; Ninham, B. W. *J. Chem. Soc., Faraday Trans. 2* **1976**, *72*, 1525.
(48) Eicke, H.-F.; Rehak, J. *Helv. Chim. Acta* **1976**, *59*, 2883.
(49) Tuzar, Z.; Stepanek, P.; Konak, C.; Kratochvil, P. *J. Colloid Interface Sci.* **1985**, *105*, 372.
(50) Assih, T.; Larche, F.; Delord, P. *J. Colloid Interface Sci.* **1982**, *89*, 35.
(51) Mitchell, D. J.; Ninham, B. W. *J. Chem. Soc., Faraday Trans. 2* **1981**, *77*, 601.
(52) Duval, M.; Picot, C. *Polymer* **1987**, *28*, 793.
(53) Lally, T. P.; Price, C. *Polymer* **1974**, *15*, 325.
(54) Sikora, A.; Tuzar, Z. *Makromol. Chem.* **1983**, *184*, 2049.
(55) Utiyama, H.; Takensaka, K.; Mizumori, M.; Fukuda, M.; Tsunashima, Y.; Kurata, M. *Macromolecules* **1974**, *7*, 515.
(56) Price, C. *Pure Appl. Chem.* **1983**, *55*, 1563.
(57) Price, C.; Chan, E. K. M.; Hudd, A. L.; Stubbersfield, R. B. *Polym. Commun.* **1986**, *27*, 196.
(58) Tuzar, Z.; Bahadur, P.; Kratochvil, P. *Makromol. Chem.* **1981**, *182*, 1751.
(59) Franta, E.; Skoulios, A.; Rempp, P.; Benoit, H. *Makromol. Chem.* **1965**, *87*, 271.
(60) Gervais, M.; Gallot, B. *Makromol. Chem.* **1973**, *174*, 193.
(61) DiMarzio, E. A.; Guttman, C. M.; Hoffman, J. D. *Macromolecules* **1980**, *13*, 1194.
(62) Gallot, B. R. M. *Adv. Polym. Sci.* **1978**, *29*, 85.
(63) Kinning, D. J.; Winey, K. I.; Thomas, E. L. *Macromolecules* **1988**, *21*, 3502.
(64) Whitmore, M. D.; Noolandi, J. *Macromolecules* **1988**, *21*, 1482.

Registry No. (S)(EO) (block copolymer), 107311-90-0; cyclopentane, 287-92-3.

Deuterium Magnetic Resonance Study of Some Liquid-Crystalline Polysiloxanes

M. Mauzac,* H. Richard, and L. Latie

Centre de Recherche Paul Pascal, Domaine Universitaire, 33405 Talence Cedex, France.
Received March 23, 1989; Revised Manuscript Received July 6, 1989

ABSTRACT: Deuterium nuclear magnetic resonance is used to study two side-chain poly(methylsiloxanes) and their corresponding low molecular weight mesogens. The compounds are selectively deuterated and are studied as a function of temperature over their mesomorphic regions. The measurement of the various quadrupolar splittings and, in some cases, of the dipolar interactions are analyzed in terms of orientational order, using a single-order parameter model. In addition, some information is given about the probability distribution of gauche conformers in the aliphatic chains of the various compounds.

1. Introduction

In previous papers[1-3] we have described the synthesis and mesogenic properties of a series of poly(methylsiloxanes) substituted by the following phenyl benzoates:

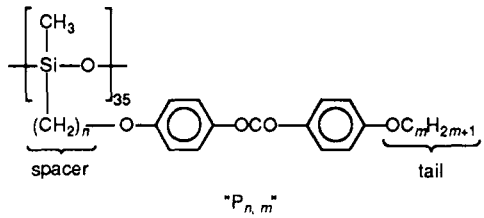

"$P_{n,m}$"

For an understanding of the relationships between structure and properties, investigations on chain conformation, molecular order, and dynamics of the mesogenic groups are necessary. Some results have been recently obtained by small-angle neutron scattering,[4] dielectric investigations,[5] and ^{13}C NMR measurements.[6] Deuterium magnetic resonance is also particularly useful and has been extensively used to study molecular structure and ordering of liquid-crystalline phases.[7-15]

In the present paper we report a ^2H NMR study of two polymers of the series $P_{4,1}$ ($n = 4$, $m = 1$) and $P_{4,8}$ ($n = 4$, $m = 8$) and of the two corresponding low molecular weight (LMW) mesogens group $M_{4,1}$ and $M_{4,8}$.

The mesogens are selectively deuterated in the spacer and in the tail. Quadrupolar and dipolar interactions are analyzed in terms of the model of Hsi et al.[7] The single-order parameter of the model and the probability of gauche conformers in the aliphatic chain are deduced. The results obtained with different labeling sites are compared, concerning both the LMW and the polymer mesogens.

2. Experimental Section

2.1. Materials. The synthesis of the deuterated mesogenic groups has been performed by using the same classical reactions described in a preceding paper.[1] The compounds are labeled

0024-9297/90/2223-0753$02.50/0